Coadsorption and Surface Forces for Selective Surfaces in Contact with Aqueous Mixtures of Oppositely Charged Surfactants and Low Charge Density Polyelectrolytes

Orlando J. Rojas,[†,‡] Per M. Claesson,[†] K. Derek Berglund,[§] and Robert D. Tilton*[,§,||]

Department of Chemistry, Surface Chemistry, Royal Institute of Technology, Drottning Kristinas väg 51, SE 100 44, Stockholm, Sweden; Institute for Surface Chemistry, P.O. Box 5607, SE 114 86 Stockholm, Sweden; Department of Chemical Engineering, Center for Complex Fluids Engineering, Carnegie Mellon University, Pittsburgh, Pennsylvania 15213; and Department of Biomedical Engineering, Carnegie Mellon University, Pittsburgh, Pennsylvania 15213

Received September 18, 2003. In Final Form: December 22, 2003

The coadsorption of a positively charged polyelectrolyte (with 10% of the segments carrying a permanent positive charge, AM-MAPTAC-10) and an anionic surfactant (sodium dodecyl sulfate, SDS) on silica and glass surfaces has been investigated using optical reflectometry and a noninterferometric surface force technique. This is a selective coadsorption system in the sense that the polyelectrolyte does adsorb to the surface in the absence of surfactant, whereas the surfactant does not adsorb in the absence of polyelectrolyte. It is found that the total adsorbed amount goes through a maximum when the SDS concentration is increased. Maximum adsorption is found when the polyelectrolyte/surfactant complexes formed in bulk solution are close to the charge neutralization point. Some adsorption does occur also when SDS is present in significant excess. The force measured between AM-MAPTAC-10-coated surfaces on approach in the absence of SDS is dominated at long range by an electrostatic double-layer force. Yet, layers formed by coadsorption from solutions containing both polyelectrolyte and surfactant generate long-range forces of an electrosteric nature. On separation, adhesive interactions are found only when the adsorbed amount is low, i.e., in the absence of SDS and in a large excess of SDS. The final state of the adsorbed layer is found to be nonhysteretic, i.e., independent of the history of the system. The conditions for formation of long-lived trapped adsorption states from mixed polymer−surfactant solutions are discussed.

Introduction

Aqueous mixtures of polymers and surfactants are found in a wide range of complex fluid technologies. Often, polymers and surfactants are included in a fluid formulation to achieve independent objectives, for example, when polymers are intended to control rheology and surfactants are intended to control capillarity. Polymers and surfactants often interact strongly in solution and therefore exert coupled effects on complex fluid properties. Ideally, polymer/surfactant mixtures may be formulated to exploit synergistic effects.

There are numerous materials formulations and applications where adsorption from polymer/surfactant mixtures to the solid−liquid interface is a critical aspect. Examples include pharmaceutical suspensions and slurries, pigment dispersal, printing and coating processes, and cleaning formulations. The effects of polymer/surfactant interactions on adsorption and surface modification remain difficult to predict. Furthermore, it is not unusual for adsorbed layers formed by coadsorption from polymer/surfactant mixtures to exist in persistent nonequilibrium states of composition and structure.[1−4] This motivates experimental investigations of coadsorption in a variety of systems, where a variety of different types of intermolecular forces may be dominant.

Coadsorption from polymer/surfactant mixtures may be categorized according to the attractive or repulsive nature of the individual two-component interactions that operate in a polymer/surfactant/surface system. In solution, the polymer/surfactant interaction may be attractive, in which case surfactant and polymer associate, or repulsive, in which case simple mixtures are formed. Yet, even in nonbinding polymer/surfactant systems, there can be subtle mixing effects. For example, the critical micelle concentration of ionic surfactants can be less in a solution of nonbinding polyelectrolyte than it is in a polyelectrolyte-free solution.[1,2]

The interaction between the surface and the polymer or the surfactant can be described as either selective or nonselective. A selective surface is one to which one of the species (polymer or surfactant), but not the other, would ordinarily adsorb from a single-component solution. Four types of systems are readily identified: Surfactant binds to polymer and surface is selective (type I) or nonselective (type II); surfactant does not bind to polymer and surface is selective (type III) or nonselective (type IV). See Velegol

* Address correspondence to Prof. Tilton. E-mail: tilton@andrew.cmu.edu.

† Royal Institute of Technology and Institute for Surface Chemistry.

‡ Present address: Department of Wood & Paper Science, North Carolina State University, Raleigh, North Carolina 27695.

§ Department of Chemical Engineering, Center for Complex Fluids Engineering, Carnegie Mellon University.

|| Department of Biomedical Engineering, Carnegie Mellon University.

(1) Velegol, S. B.; Tilton, R. D. *J. Colloid Interface Sci.* **2002**, *249*, 282−289.

(2) Velegol, S. B. *Tuning Interfacial and Bulk Self-Assembly of Ionic Surfactants via Counterions and Non-Binding Polyelectrolytes;* Ph.D. Dissertation, Carnegie Mellon University: Pittsburgh, PA, 2000.

(3) Velegol, S. B.; Tilton, R. D. *Langmuir* **2001**, *17*, 219−227.

(4) Braem, A. D.; Prieve, D. C.; Tilton, R. D. *Langmuir* **2001**, *17*, 883−890.

10.1021/la035752w CCC: $27.50
Published on Web 02/27/2004

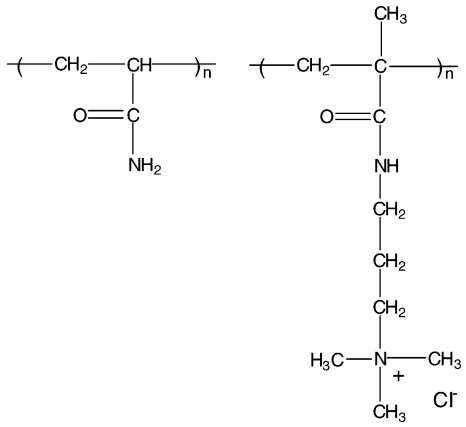

Figure 1. Molecular structure of the AM (left) and MAPTAC (right) repeat units in the AM-MAPTAC-10 random copolymer.

and Tilton,[3] Braem and co-workers,[4] and references therein for examples of each type.

The current investigation considers a type I system, where the polymer/surfactant binding is driven by electrostatic attraction between anionic sodium dodecyl sulfate (SDS) surfactants and cationic AM-MAPTAC-10 polyelectrolytes. AM-MAPTAC-10 is a random copolymer of nonionic acrylamide (AM) and cationic (3-(methylpropionamido)propyl)trimethylammonium chloride (MAPTAC), having a 9:1 ratio of nonionic monomers to cationic quaternary amine monomers (Figure 1). The surface, negatively charged silica or glass, is selective for AM-MAPTAC-10 adsorption. SDS does not adsorb to these surfaces. Here we consider coadsorption from mixed solutions rather than the effect of exposing preadsorbed polymer layers to a surfactant solution. This distinction is important. As will be noted in the Results and Discussion section, adsorbed polyelectrolyte layers respond quite differently to changes in composition of a mixed polyelectrolyte/surfactant solution than they do to surfactant concentration changes in a polyelectrolyte-free solution.

In several type I coadsorption systems previously studied, the composition and structure of the adsorbed layers was found to depend on the order in which the surface was exposed to surfactants and polymers.[1,3,5−14] This path-dependent coadsorption is referred to as hysteretic and is characterized by persistent nonequilibrium states at interfaces. It probably is at least partially responsible whenever one observes that the order of component addition or the mixing conditions affect the successful formulation of a colloidal complex fluid.

In this paper, we discuss how the amount of adsorption and the layer structure depend on the surfactant concentration. We also discuss factors that may determine whether a coadsorption system behaves in a hysteretic or a reversible manner. Using a combination of optical reflectometry and surface force measurements, we will show that the SDS/AM-MAPTAC-10/silica (glass) system is not hysteretic as long as some SDS is present in solution. Although AM-MAPTAC-10 adsorption on silica is effectively irreversible in the absence of surfactant, mixed adsorbed layers respond reversibly to changes in the concentration of SDS in a mixed AM-MAPTAC-10/SDS solution.

In the absence of SDS, adsorbed AM-MAPTAC-10 layers are relatively thin, with regions of the surface accessible to bridging chains from opposite surfaces. Complexation with SDS, at concentrations below the critical micelle concentration (CMC), leads to the formation of thick layers that contain large amounts of adsorbed material. In an excess of SDS, adsorbed layers are again sparse but the SDS-saturated AM-MAPTAC-10 chains appear to be rather extended on the surface under these conditions. Surface interactions are adhesive in the absence of SDS or in an excess of SDS. Adhesion is eliminated in the presence of SDS at concentrations below the CMC, even under conditions where polyelectrolyte/surfactant binding leads to decreased solubility and the formation of large aggregates in solution.

Experimental Section

Materials. The AM-MAPTAC-10 sample used in this work had a molecular weight of approximately 1×10^6. It was synthesized and kindly donated by Laboratoire de Physico Chimie Macromoleculaire, Paris. The synthesis is analogous to that previously described for acryl(*N*,*N*,*N*-trimethyl)aminoethyl chloride-AM.[15] Sodium dodecyl sulfate (SDS, 99% pure) was purchased from Sigma and used as received. Sodium chloride (Suprapure grade) was purchased from Merck and used as received. All water was purified by reverse osmosis, followed by treatment with either a Millipore MilliQ Plus unit (reflectometry measurements) or a Millipore MilliQ 185 unit (force measurements and dynamic light-scattering measurements). Samples for all measurements, unless otherwise noted, were made in unbuffered aqueous solutions containing 0.1 mM NaCl and 50 ppm (w/v) AM-MAPTAC-10. The electrostatic binding of SDS to AM-MAPTAC-10 in solution is strong. The critical aggregation concentration (CAC) is estimated to be 0.01 × CMC or approximately 0.08 mM.[16]

Optical reflectometry experiments were conducted with silicon wafers (Valley Design Corp.) that had been oxidized for 20−25 min in 1000 °C air to produce approximately 30 nm thick oxide layers on their surfaces. Precise oxide layer thicknesses were measured by scanning angle optical reflectometry at the start of each experiment. The wafer cleaning procedure described previously[12] leaves these surfaces negatively charged and perfectly wetted by water. Cleaned wafers were stored in water and rinsed profusely before being mounted wet in the reflectometer.

For surface force measurements, flame polished glass surfaces were prepared by melting the end of a borosilicate glass rod (DIN.ISO 3585, known commercially as Pyrex, obtained from Wernerglas) in a butane−oxygen flame until a spherical drop of approximately 2 mm radius formed and then cooling at room temperature. This procedure produces clean, smooth surfaces with 0.1 nm roughness.[17]

Dynamic Light Scattering. The size of AM-MAPTAC-10 and its complexes with SDS in solution were examined using a Brookhaven laser light-scattering goniometer and model BI-9000AT digital autocorrelator. Samples for dynamic light scattering were prepared with filtered water in a laminar flow cabinet and equilibrated at 23 °C. Autocorrelation functions were

(5) Braem, A. D. *Colloidal and Interfacial Phenomena in Polymer/Surfactant Mixtures;* Ph.D. Dissertation, Carnegie Mellon University: Pittsburgh, PA, 2001.
(6) Furst, E. M.; Pagac, E. S.; Tilton, R. D. *Ind. Eng. Chem. Res.* **1996**, *35*, 1566−1574.
(7) Neivandt, D. J.; Gee, M. L.; Tripp, C. P.; Hair, M. L. *Langmuir* **1997**, *13*, 2519−2526.
(8) Pagac, E. S.; Prieve, D. C.; Tilton, R. D. *Langmuir* **1998**, *14*, 2333−2342.
(9) Dedinaite, A.; Claesson, P. M.; Bergström, M. *Langmuir* **2000**, *16*, 5257−5266.
(10) Dedinaite, A.; Claesson, P. M. *Langmuir* **2000**, *16*, 1951−1959.
(11) Braem, A. D.; Biggs, S.; Prieve, D. C.; Tilton, R. D. *Langmuir* **2003**, *19*, 2736−2744.
(12) Berglund, K. D.; Przybycien, T. M.; Tilton, R. D. *Langmuir* **2003**, *19*, 2705−2713.
(13) Berglund, K. D.; Przybycien, T. M.; Tilton, R. D. *Langmuir* **2003**, *19*, 2714−2721.
(14) Berglund, K. D.; Timko, A.; Przybycien, T. M.; Tilton, R. D. *Prog. Colloid Polym. Sci.* **2003**, *122*, 56−66.
(15) Mabire, F.; Audebert, R.; Quivoron, C. *Polymer* **1984**, 1317−1322.
(16) Claesson, P. M.; Dedinaite, A.; Fielden, M.; Kjellin, M.; Audebert, R. *Prog. Colloid Polym. Sci.* **1997**, *106*, 24−33.
(17) Ederth, T.; Claesson, P.; Liedberg, B. *Langmuir* **1998**, *14*, 4782−4789.

analyzed by the CONTIN method,[18,19] and the resulting relaxation time distributions were converted to intensity-weighted distributions of apparent hydrodynamic diameter using the Stokes−Einstein equation for spheres.

Optical Reflectometry. We used optical reflectometry to measure the extent and reversibility of adsorption. A detailed description of the technique as we employ it is available elsewhere.[20] We used the instrument described by Furst and co-workers,[6] as modified according to Velegol and co-workers.[3,21] The oxidized silicon wafer served as one wall of a rectangular slit flow cell. Solutions were pumped by a syringe pump, making one pass through the flow cell, without recirculation, at a wall shear rate of approximately 2 s^{-1}. Besides the oxidized silicon wafer, all materials that contacted the solution were either stainless steel, Teflon, fluorinated elastomer O-rings, or acid-cleaned glass. After mounting a wafer in the flow cell, we monitored the reflectivity for approximately 20 min while flowing a 0.1 mM NaCl solution, as a check against surface active impurities. The temperature was controlled at 25 ± 0.1 °C.

Steady-state surface excess concentrations were determined by the scanning angle method of recording the reflection coefficient for p-polarized light, R_p, as a function of incident angle near the Brewster angle. We evaluated the optical properties of the adsorbed layers using the homogeneous two-layer optical model,[20] where the bulk solution and bulk silicon are separated by an adsorbed layer of unknown thickness and refractive index and an oxide layer of known thickness and refractive index. The refractive indices for silicon and for silicon oxide at the 632.8 nm HeNe laser wavelength are 3.882 + 0.019i and 1.46, respectively. The refractive index of the bulk solutions were calculated based on their composition using known refractive index increments.

Using the Abeles matrix method[22] to numerically evaluate the two-layer optical model, we used χ^2 minimization to fit each measured reflectivity profile to obtain an optical average thickness, d_{av}, and an optical average refractive index, n_{av}, for the adsorbed layer. From these parameters, we calculated the *effective* optical thickness of the adsorbed layer $d_{av}(n_{av} - n_o)$, where n_o is the bulk solution refractive index. The effective optical thickness is related to the surface excess concentration Γ_i of each species i in a mixed adsorbed layer by

$$d_{av}(n_{av} - n_o) = \sum_i \Gamma_i(dn/dC_i) \quad (1)$$

where dn/dC_i is the refractive index increment of species i. The refractive index increments determined by differential refractometry for SDS and for AM-MAPTAC-10 are 0.12 and 0.13 cm^3/g, respectively. Since optical reflectometry does not distinguish the relative adsorbed amounts in a mixed layer, we report both the effective optical thickness of the layer and the apparent AM-MAPTAC-10 surface excess concentration, calculated from the effective optical thickness by assuming the layer contains only the polyelectrolyte. Because of the similarity of the refractive index increments, this only slightly underestimates (at most by 8%) the total surface excess concentration for mixed layers of SDS and AM-MAPTAC-10.

Surface Force Measurements. We used the MASIF bimorph surface force apparatus to measure forces between opposing glass surfaces. This instrument has been described in detail elsewhere.[23] The MASIF technique provides a measure of interaction forces between two hard, smooth surfaces of known geometry. In this case, we measured the force between two spheres. The upper sphere was mounted to a piezoelectric tube, while the lower sphere was mounted to a piezoelectric bimorph spring. The separation between the two spheres was varied continuously by applying a triangular voltage wave to the piezoelectric tube. The bimorph spring produced a charge when it bent in response to the force acting between the two spheres. This charge was amplified to continuously monitor the spring deflection as a function of the upper sphere displacement. When the two surfaces came into contact, the motion of the upper, driven surface was directly transmitted to the bimorph spring, thus allowing the spring to be calibrated against piezoelectric tube displacement.

The bimorph spring deflection data were converted to force via Hooke's Law, using the bimorph spring constant measured at the end of each experiment. For analysis, the forces were normalized by the harmonic mean radius of the upper and lower spheres, $R = 2R_{up}R_{low}/(R_{up} + R_{low})$. Typically, the radii of upper and lower spheres were the same to within approximately 5%.

The glass spheres were enclosed in a 10 mL stainless steel chamber fitted with syringe ports for liquid exchange. Whenever the solution in the chamber was changed to measure forces under different conditions, the surface separation was set to approximately 0.5 mm and the chamber was drained. This left a small drop of solution to span the gap and wet both hydrophilic surfaces. The chamber was then refilled with the new solution that had been prepared earlier. This procedure ensured that all bulk solutions were initially well mixed and preequilibrated and that a three-phase contact line never swept across the part of either surface where forces were measured.

Hydrodynamic effects on force measurements were addressed by measuring force profiles at different driving rates (from 5 to 200 nm/s). Typically, the force profiles reported herein were obtained at driving rates on the order of 5−15 nm/s, where force profiles did not depend on driving rate. Hydrodynamic forces therefore contributed negligibly to the total force under these conditions.

Results and Discussion

Bulk Solution Binding Behavior. In the following, SDS concentrations are reported as a multiple of the CMC (8.1 mM) that is measured in 0.1 mM NaCl solutions that do not contain the polyelectrolyte. The actual concentration that marks the appearance of free micelles in an AM-MAPTAC-10 solution, CMC_p, is not necessarily the same as the CMC.

The SDS/AM-MAPTAC-10 system displayed the characteristic tendency of oppositely charged polyelectrolytes and surfactants to form turbid mixtures at surfactant concentrations near the point of complex neutralization, whereupon the solubility decreases and large aggregates form. Mixtures containing 50 ppm AM-MAPTAC-10/0.1 × CMC SDS/0.1 mM NaCl formed turbid homogeneous solutions. No macroscopic phase separation was observed over more than an 8-week period, implying that these mixtures were colloidally stable suspensions of polyelectrolyte−surfactant aggregates.

Dynamic light-scattering experiments were performed on AM-MAPTAC-10 samples containing 0, 0.5, 1, and 2 × CMC SDS. These were transparent. The 50 ppm AM-MAPTAC-10/2 × CMC SDS/0.1 mM NaCl solutions had a bimodal size distribution dominated by species having apparent hydrodynamic diameters of 75 and 3 nm. As shown in Figure 2, the smaller scatterers accounted for 7% of the cumulative scattering intensity. This indicates that AM-MAPTAC-10/SDS complexes coexisted with free SDS micelles when the total SDS concentration was 2 × CMC. Thus, the chemical potential of SDS monomers was fixed at a value corresponding to CMC_p.

At a total SDS concentration of 1 × CMC, the intensity-weighted size distribution was dominated by a species having a 73 nm mean apparent hydrodynamic diameter and the peak corresponding to free micelles only accounted for 1% of the cumulative intensity. The appearance of some free micelles at a total SDS concentration of 1 × CMC indicates that CMC_p < CMC. (Note that counterion mass action effects can decrease ionic surfactant CMC's in the presence of polyelectrolytes in solution.[1,2])

(18) Provencher, S. W. *Comput. Phys. Commun.* **1982**, *27*, 213.
(19) Provencher, S. W. *Comput. Phys. Commun* **1982**, *27*, 229.
(20) Tilton, R. D. *Scanning Angle Reflectometry and Its Application to Polymer Adsorption and Coadsorption with Surfactants;* Farinato, R. S., Dubin, P. L., Eds.; John Wiley & Sons: New York, 1999; p 331.
(21) Velegol, S. B.; Fleming, B. D.; Biggs, S.; Wanless, E. J.; Tilton, R. D. *Langmuir* **2000**, *16*, 2548−2556.
(22) Azzam, R. M. A.; Bashara, N. M. *Ellipsometry and Polarized Light;* North-Holland: Amsterdam, 1977.
(23) Parker, J. L. *Langmuir* **1992**, *8*, 551−556.

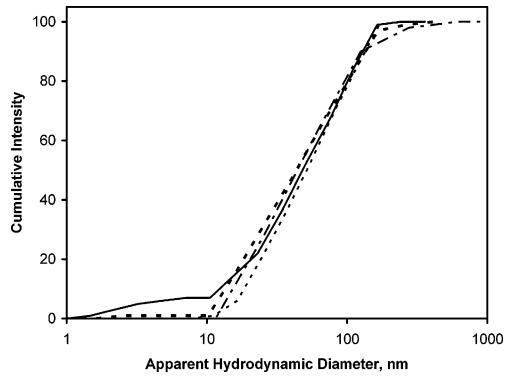

Figure 2. Cumulative scattered light intensities for different apparent hydrodynamic diameters of AM-MAPTAC-10 (50 ppm polymer concentration) and its complexes with SDS at 23 °C. The different distributions correspond to 0 × CMC SDS (short dashes), 0.5 × CMC SDS (dot−dash), 1 × CMC SDS (long dashes), and 2 × CMC SDS (solid line).

At 0.5 × CMC, the distribution was monomodal with a mean apparent hydrodynamic diameter of 80 nm. The AM-MAPTAC-10 solutions that were used for dynamic light-scattering measurements in the absence of SDS were made with 10 mM NaCl to screen long-range electrostatic interactions that contribute a slow mode to the autocorrelation function. The mean apparent hydrodynamic diameter of AM-MAPTAC-10 in SDS-free NaCl solution was 78 nm.

The similarity of the apparent sizes for AM-MAPTAC-10/SDS complexes that form at SDS concentrations greater than or equal to 0.5 × CMC to the size of AM-MAPTAC-10 in SDS-free solution indicates that those complexes each contain a single AM-MAPTAC-10 chain.

Extent of Adsorption. Since coadsorption from mixtures of polymers and surfactants is often strongly hysteretic, we compared extents of adsorption for both one-step and sequential coadsorption experiments. In one-step experiments, one polyelectrolyte/surfactant mixture of predetermined composition was allowed to adsorb to a fresh surface. In a sequential coadsorption experiment, the fresh surface was first exposed to a 50 ppm AM-MAPTAC-10/0.1 mM NaCl solution that contained no SDS. Then, that preadsorbed AM-MAPTAC-10 layer was sequentially exposed to solutions that each contain 50 ppm AM-MAPTAC-10/0.1 mM NaCl but with increasing concentrations of SDS. The final step of the sequential coadsorption experiment was to rinse the adsorbed layer with 0.1 mM NaCl solution that contained neither SDS nor AM-MAPTAC-10.

Figure 3 shows that the extent of coadsorption did not depend on the adsorption sequence. The amount of adsorption after the final rinse with 0.1 mM NaCl solutions is the same as the amount of AM-MAPTAC-10 that adsorbs in the absence of SDS. Since polyelectrolyte/surfactant binding is reversible, the adsorbed remnant after the rinse is irreversibly adsorbed AM-MAPTAC-10. Irreversible adsorption over practical laboratory time scales is typical of macromolecule adsorption,[24−29] including electrostatically driven polyelectrolyte adsorption to oppositely charged surfaces.[3]

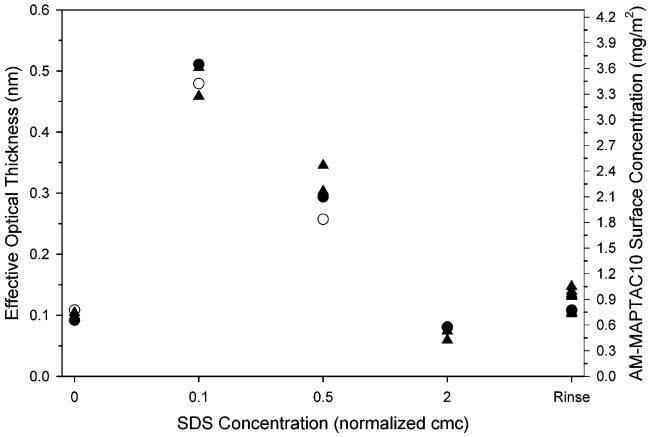

Figure 3. Total extent of adsorption from solutions containing 50 ppm AM-MAPTAC-10, 0.1 mM NaCl, and varying concentrations of SDS. The apparent AM-MAPTAC-10 surface excess concentration is calculated from the effective optical thickness by assuming that the layer contains only the polyelectrolyte. (○ and ●) Results of two independent sequential adsorption experiments where the SDS concentration was increased from zero to 2 × cmc at a fixed 50 ppm AM-MAPTAC-10 concentration. (▲) Results from separate one-step coadsorption experiments, each with 50 ppm AM-MAPTAC-10. The uncertainty in the apparent AM-MAPTAC-10 surface excess concentration is ±0.05 mg/m^2. Protocols for one-step and sequential coadsorption experiments are explained in the text.

In the absence of SDS, AM-MAPTAC-10 adsorbed to approximately 0.8 mg/m^2 on the silica surface, corresponding to approximately 2100 nm^2 per chain or one chain occupying a 50 nm diameter area. This is comparable to the apparent hydrodynamic diameter of AM-MAPTAC-10 in solution.

The total extent of adsorption increased significantly (to 3.6 mg/m^2) as the SDS concentration was increased to 0.1 × CMC, remained high (2.2 mg/m^2) as the SDS concentration was increased further to 0.5 × CMC, but returned at 2 × CMC to a lower value (0.6 mg/m^2) than that attained in the absence of SDS. Recall that these adsorbed amounts represent a sum of SDS and AM-MAPTAC-10 adsorption, expressed as an apparent amount of AM-MAPTAC-10 adsorption. Intensity losses due to light scattering from the turbid solution in the reflectometry flow cell introduce some uncertainty in the total extent of adsorption at 0.1 × CMC. Turbidity was not a problem in any of the other solutions. Thus, the enhancement of adsorption at 0.5 × CMC, relative to adsorption from SDS-free solution, confirmed the elevated surface activity of AM-MAPTAC-10/SDS complexes in solutions that do not contain free micelles.

The lack of any dependence on the adsorption sequence demonstrates that the adsorbed layer responds reversibly to changes in solution composition when SDS is present. Nevertheless, the data after the final rinse with 0.1 mM NaCl solution demonstrate that AM-MAPTAC-10 adsorbs irreversibly once SDS is removed from the system. It should be noted that SDS does not adsorb to silica in the absence of polymers, so there is no chance that the residual left on the surface after rinsing was SDS. The insensitivity of the SDS/AM-MAPTAC-10 layers to adsorption history is in sharp contrast to the great sensitivity displayed by mixed layers of cationic polylysine and cationic hexadecyltrimethylammonium halide surfactants on silica.[1,3]

(24) Fleer, G. J.; Cohen Stuart, M. A.; Scheutjens, J. M. H. M.; Cosgrove, T.; Vincent, B. *Polymers at Interfaces;* Chapman & Hall: London, 1993.

(25) Schneider, H. M.; Frantz, P.; Granick, S. *Langmuir* **1996**, *12*, 994−996.

(26) Konstadinidis, K.; Prager, S.; Tirrell, M. *J. Chem. Phys.* **1992**, *97*, 7777−7780.

(27) Norde, W.; MacRitchie, F.; Nowicka, G.; Lyklema, J. *J. Colloid Interface Sci.* **1986**, *112*, 447−456.

(28) O'Shaughnessy, B.; Vavylonis, D. *Eur. Phys. J. E* **2003**, *11*, 213−230.

(29) Pagac, E. S.; Prieve, D. C.; Solomentsev, Y.; Tilton, R. D. *Langmuir* **1997**, *13*, 2993−3001.

The origins for this lack of history dependence will be discussed below.

A comment is warranted on the small increase in adsorption that occurred when mixed layers were rinsed with 0.1 mM NaCl solution. This behavior has been observed previously in systems where the effect of surfactant dilution is to increase the polymer surface activity. The additional adsorption occurs as the dilute front passes over the surface during the first stage of rinsing under laminar Poiseuille flow conditions, as discussed at some length elsewhere.[13]

In light of the aggregation behavior in solution, the extensive adsorption from solutions containing 0.1 × CMC SDS should be attributed to the buildup of a layer of aggregates adsorbed from a colloidally stable but thermodynamically unstable solution. A similar effect has been noted previously for adsorption at the air−water interface of SDS mixtures with lysozyme protein.[30] In a separate study with AM-MAPTAC-1, a similar polyelectrolyte having a 99:1 ratio of nonionic to cationic monomers, Rojas and co-workers studied the desorption of *preadsorbed* polyelectrolytes from silica surfaces into SDS solutions that contained no polyelectrolyte.[31] All SDS solutions examined, including ones below the CMC, were found to promote polyelectrolyte desorption. Similar behavior was observed for AM-MAPTAC-10 preadsorbed on negatively charged mica surfaces.[32] This contrasts with the current results obtained when surfaces were exposed to mixed solutions. Although dilute SDS solutions (containing no AM-MAPTAC) were capable of washing preadsorbed AM-MAPTAC polyelectrolytes from the silica surface, polyelectrolyte−surfactant aggregation under low solubility conditions dictates the surface coverage in the presence of a mixed solution of AM-MAPTAC-10 and 0.1 × CMC SDS. The practical implication of this observation is that one must be careful to consider the full composition of the bulk solution when considering the effects of surfactant concentration on the structure and composition of an adsorbed polyelectrolyte layer. The presence or absence of polyelectrolyte in solution has a major effect. The layer formed by deposition from an unstable solution responded reversibly to changes in the bulk solution composition, as shown by the sequential coadsorption results in Figure 3.

The 50 ppm AM-MAPTAC-10/0.5 × CMC SDS/0.1 mM NaCl mixture and the 50 ppm AM-MAPTAC-10/2 × CMC SDS/0.1 mM NaCl mixture are thermodynamically stable solutions of polyelectrolyte/surfactant complexes. The very large adsorbed amount at 0.5 × CMC, approximately three times the total adsorbed amount of AM-MAPTAC-10 attained in the absence of SDS, cannot be attributed to the thermodynamic instability of the bulk solution. Given the size of AM-MAPTAC-10 and its complexes in solution, such a layer must be thick. A plausible structure for the layer under these conditions where the AM-MAPTAC-10/SDS binding is not yet saturated is a three-dimensional SDS-linked network of AM-MAPTAC-10 chains. We note that a recent small-angle neutron-scattering study of AM-MAPTAC-10/SDS complexes in bulk solution suggests that the aggregates formed with a slight excess of SDS in solution consist of smaller units, most likely rodlike SDS micelles associated with the polyelectrolyte,[33] i.e., a structure similar to that suggested here for the adsorbed layer formed from a 0.5 × CMC SDS solution.

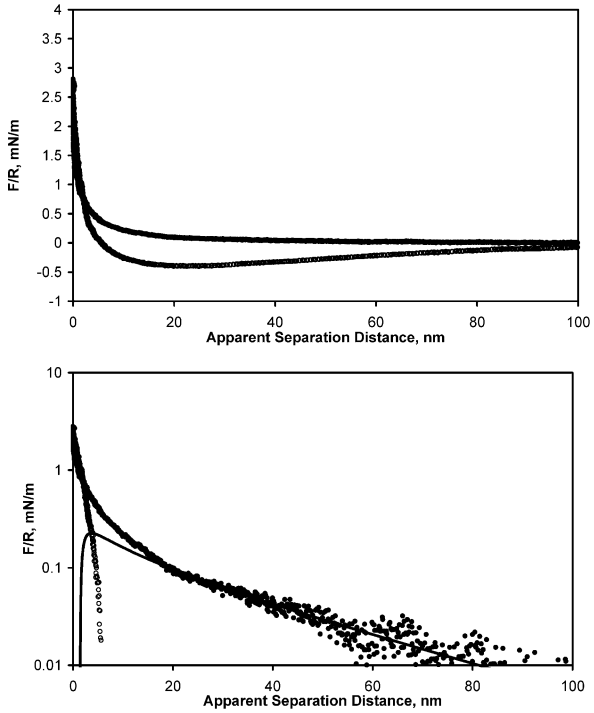

Figure 4. Linear (a) and semilogarithmic (b) plots of the interaction force normalized by radius as a function of apparent surface separation of glass spheres across aqueous 50 ppm AM-MAPTAC-10 solution (0.1 mM NaCl background electrolyte). Filled and open circles represent the force profiles obtained upon approach and separation, respectively. The surface driving rate was small enough that hydrodynamic effects were negligible. In the semilogarithmic plot (b) the inward curve is shown together with a fit to DLVO theory with constant surface charge boundary condition (solid line). The following parameters were used in the fitting: apparent surface potential $\Psi_0 = 33$ mV; Debye length $\kappa^{-1} = 30$ nm; Hamaker constant $A = 1 \times 10^{-20}$ J. Data collected at 22 °C after more than 24 h equilibration time.

Surface Forces. The forces between opposing glass surfaces in 0.1 mM NaCl solution were consistent with double-layer repulsion between spherical surfaces of −80 mV surface potential (not shown). At short range, a steep repulsion overwhelmed the van der Waals attraction, resulting in a purely repulsive interaction at all separation distances. There was no hysteresis between forces measured on approach and on separation of the two surfaces. The observed force curves were typical of previously reported ones for glass surfaces in simple electrolyte solutions.[23]

Figure 4 shows the normalized force as a function of separation distance for two glass surfaces in a 50 ppm AM-MAPTAC-10/0.1 mM NaCl solution. The adsorbed layer was allowed to equilibrate for 1 day. The long-range force measured on approach was consistent with the DLVO force for similarly charged spheres with a 33 mV surface potential and a Debye length, κ^{-1}, of 30 nm that corresponds well with the ionic strength of the electrolyte solution (0.1 mM NaCl). A Hamaker constant of 1×10^{-20} J, appropriate for glass surfaces interacting in water, was assumed when calculating the DLVO force. The extent of adsorption measured by optical reflectometry would indicate that the underlying glass surface charge density has been overcompensated by the 10% quaternary charge density AM-MAPTAC-10, rendering the interface with a net positive charge, a conclusion also drawn by Poptoshev and Claesson.[34]

(30) Sun, M. L.; Tilton, R. D. *Colloids Surf. B: Biointerfaces* **2001**, *20*, 281.
(31) Rojas, O. J.; Ernstsson, M.; Neuman, R. D.; Claesson, P. M. *J. Phys. Chem. B* **2000**, *104*, 10032−10042.
(32) Rojas, O. J.; Ernstsson, M.; Neuman, R. D.; Claesson, P. M. *Langmuir* **2002**, *18*, 1604−1612.
(33) Bergström, M.; Kjellin, M.; Claesson, P. M.; Grillo, I. Submitted for publication.

The measured force became more repulsive than the DLVO force at an apparent separation distance of approximately 15 nm. This may be attributed to electrosteric interactions between opposing layers of adsorbed polyelectrolytes. We note that in the study of Poptoshev and Claesson, the interactions between AM-MAPTAC-10-coated glass surfaces were studied at different AM-MAPTAC-10 concentrations. In that work the AM-MAPTAC-10 concentration was first 1 ppm and then subsequently increased to 50 ppm. The surface potential was 21 mV at 50 ppm, slightly lower than the 33 mV reported here. A more significant difference is that no long-range steric repulsion was observed when the adsorbed layer was formed by first allowing the polymer to adsorb from a 1 ppm solution and then subsequently increasing the AM-MAPTAC-10 concentration to 50 ppm. In contrast, when the adsorption layer was formed directly from the 50 ppm solution, the steric interaction extends to an apparent distance of about 20 nm (Figure 4). Hence, the adsorbed polyelectrolyte layer structure is history dependent with a more extended structure being formed when the initial adsorption is allowed to occur from a more concentrated solution. The rationale for this is that at the higher bulk concentration the adsorption rate is faster, which reduces the available time for reconformation before neighboring space on the surface is occupied by another adsorbing polyelectrolyte. The persistence of history-dependent adsorbed layer states, in the absence of surfactant, is consistent with the effectively irreversible adsorption of polyelectrolytes on oppositely charged surfaces.

For the DLVO force calculation, we assumed that the electrostatic double-layer force and the van der Waals force both originated at the zero apparent separation distance. It is not possible to know the absolute separation distance when using the noninterferometric surface force apparatus. Because of this uncertainty, the 33 mV value reported for the surface potential has little quantitative significance. The DLVO plot is shown simply to illustrate that the decay length of the long-range force is consistent with long-range electrostatic double-layer repulsion.

When separating the surfaces, a broad adhesive well having a depth of −0.5 mN/m was located at an apparent separation distance of approximately 20 nm in Figure 4. On average, the depth of the adhesive minimum was −0.4 ± 0.1 mN/m in the absence of SDS. This adhesion is attributed to cationic AM-MAPTAC-10 chains bridging between the two negatively charged glass surfaces. For the less extended adsorbed layers formed by increasing the AM-MAPTAC-10 stepwise to 50 ppm, a stronger and more long-ranged attraction was observed.[34] This is entirely consistent with bridging as the origin of the attraction.

It is interesting to note that upon separation the force profile does not show the typical jump out of contact. This situation occurs when the applied negative force exceeds the adhesion force and the force gradient exceeds the spring constant. In the present case, the attractive forces decay gradually up to an apparent surface separation on the order of 100 nm. Despite the fact that during the approach no polymer bridging takes place, it appears that after the surfaces reach contact, polymer chains interpenetrate the adsorbed layers of both surfaces. As a result polymer bridging is established and the adhesion observed during retraction of the surfaces involves the gradual unfolding and extension of polymer chains.

(34) Poptoshev, E.; Claesson, P. M. *Langmuir* **2002**, *18*, 1184−1189.

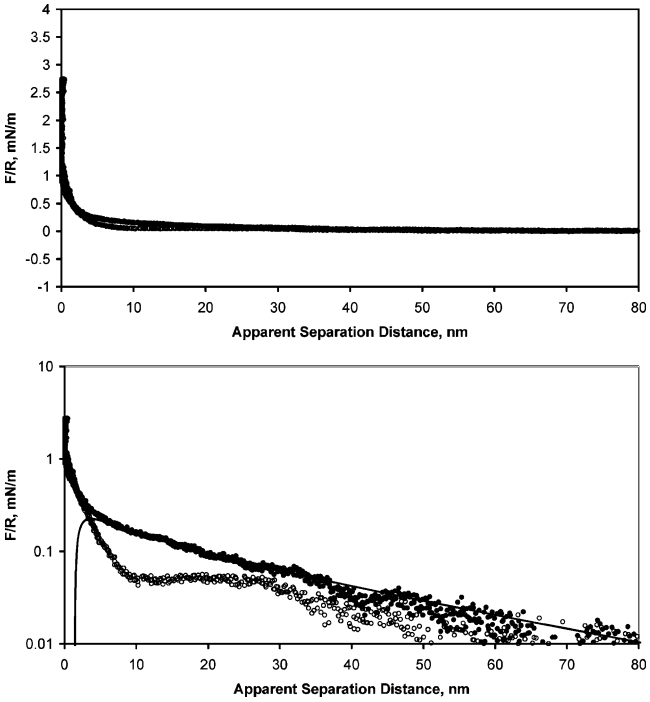

Figure 5. Linear (a) and semilogarithmic (b) plots of the interaction force normalized by radius as a function of apparent surface separation of glass spheres across aqueous 50 ppm AM-MAPTAC-10 solution in the presence of 0.1 × CMC SDS (0.1 mM NaCl background electrolyte). Filled and open circles represent the force profiles obtained upon approach and separation, respectively. In the semilogarithmic plot (b) the inward curve is shown together with a fit to DLVO theory with constant surface charge boundary condition (solid line). The following parameters were used in the fitting: apparent surface potential $\Psi_0 = 33$ mV; Debye length $\kappa^{-1} = 30$ nm; Hamaker constant $A = 1 \times 10^{-20}$ J. Data collected at 22 °C after more than 24 h equilibration time.

Glass surfaces immersed in turbid 50 ppm AM-MAPTAC-10/0.1 × CMC SDS/0.1 mM NaCl solutions provided the normalized force versus distance relationship plotted in Figure 5. The long-range forces could again be said to be consistent with DLVO interaction for an ionic strength of 0.1 mM (again with an apparent surface potential of 33 mV). The measured forces became more repulsive than the DLVO force at an apparent separation distance of nearly 10 nm. At this SDS concentration the ratio of total anionic surfactant charges to total cationic polyelectrolyte charges is 14:1. The turbidity of the solution indicates that the AM-MAPTAC-10 is nearly neutralized by bound SDS; so one may assume that one SDS is bound per quaternary charge on AM-MAPTAC-10. This would suggest that there is approximately a 13:1 excess of SDS in the system, leaving most of the SDS free as monomers in solution. At 0.1 × CMC, this corresponds to a 0.8 mM contribution from SDS to the total ionic strength. Thus, the apparent agreement with the long-range double-layer repulsion for 0.1 mM ionic strength is suggested to be fortuitous.

The optical reflectometry data at 0.1 × CMC indicated a large increase in the total extent of adsorption. The forces measured in the 50 ppm AM-MAPTAC-10/0.1 × CMC SDS/0.1 mM NaCl solutions, which form colloidally stable suspensions of aggregates, should thus be attributed to compression of a thick layer of aggregates.

One of the most significant differences between the 50 ppm AM-MAPTAC-10/0.1 × CMC SDS/0.1 mM NaCl system and the SDS-free system was the disappearance of adhesion. There was hysteresis, but no adhesion, in the

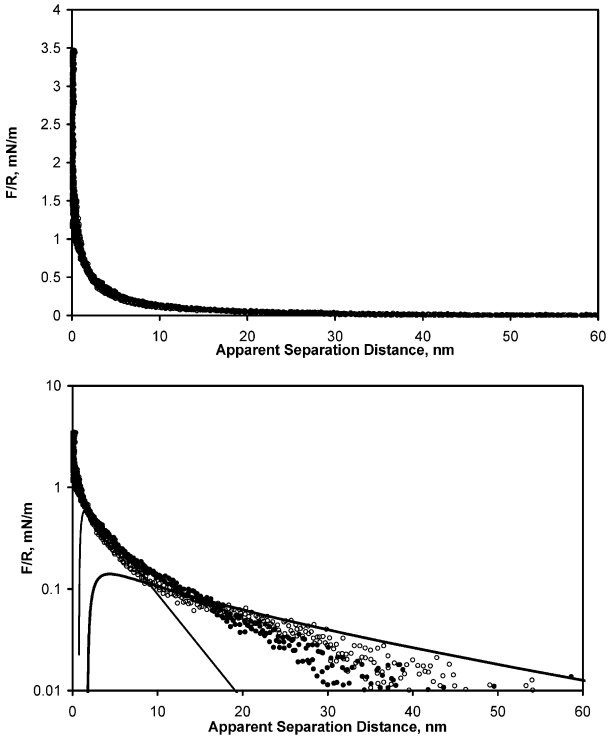

Figure 6. Linear (a) and semilogarithmic (b) plots of the interaction force normalized by radius as a function of apparent surface separation of glass spheres across aqueous 50 ppm AM-MAPTAC-10 solution in the presence of 0.5 × CMC SDS (0.1 mM NaCl background electrolyte). Filled and open circles represent the force profiles obtained upon approach and separation, respectively. In the semilogarithmic plot (b) the experimental curves are shown together with two extreme fits to DLVO theory using constant surface charge boundary conditions. In one case the ionic strength is taken to equal the NaCl concentration, 0.1 mM (solid line with small slope). In the other case, the ionic strength is taken to be the sum of the NaCl and total SDS concentrations, 4.1 mM (steep solid line). Data collected at 22 °C after more than 24 h equilibration time.

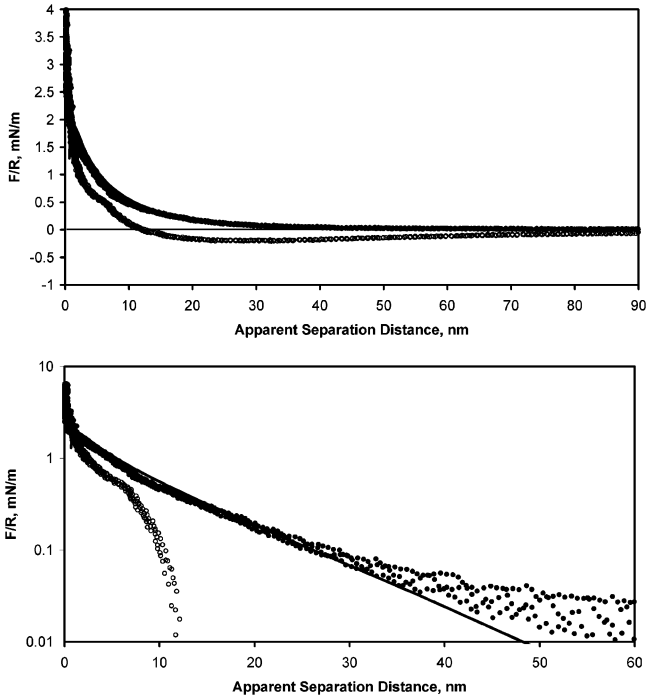

Figure 7. Linear (a) and semilogarithmic (b) plots of the interaction force normalized by radius as a function of apparent surface separation of glass spheres across aqueous 50 ppm AM-MAPTAC-10solution in the presence of 2 × CMC SDS (0.1 mM NaCl background electrolyte). Filled and open circles represent the force profiles obtained upon approach and separation, respectively. In the semilogarithmic plot (b) the inward curve is shown together with a fit to DLVO theory with constant surface charge boundary condition (solid line). The following parameters were used in the fitting: apparent surface potential $\Psi_0 = 33$ mV; Debye length $\kappa^{-1} = 30$ nm; Hamaker constant $A = 1 \times 10^{-20}$ J. Data collected at 22 °C after more than 24 h equilibration time.

50 ppm AM-MAPTAC-10/0.1 × CMC SDS/0.1 mM NaCl system. Viewed on the semilogarithmic scale, the force curve measured on separation shows a plateau between 10 and 30 nm apparent separation distance. This hysteresis may originate from intermingling of unsaturated AM-MAPTAC-10 chains with SDS molecules that are contained within the opposing adsorbed layer as well as removal of some SDS during compression.

The normalized forces between two glass surfaces immersed in a 50 ppm AM-MAPTAC-10/0.5 × CMC/0.1 mM NaCl solution are plotted in Figure 6. These data cannot be fitted to the DLVO interaction in a meaningful way. Two cases representing extremes of possible ionic strengths are shown for comparison. In one case, the ionic strength is taken to equal the NaCl concentration, 0.1 mM. In the other case, the ionic strength is taken to be the sum of the NaCl and total SDS concentrations, 4.1 mM. Neither is able to fit the data satisfactorily. Again, it is most likely that an electrosteric interaction, namely, the compression of a mixed layer with a large amount of adsorbed material, is the dominant feature of the force curve throughout the range plotted. As was the case for mixtures containing 0.1 × CMC SDS, there was no adhesion upon separation of the surfaces. The hysteresis at 0.5 × CMC was less than that at 0.1 × CMC.

Figure 7 shows the normalized force curves for glass spheres interacting across a 50 ppm AM-MAPTAC-10/2 × CMC SDS/0.1 mM NaCl solution. Again, the long-range data cannot be fitted to the DLVO force in a meaningful way. The best attempt to match the data to the DLVO model is with an ionic strength of 1.0 mM, but this must be considered to be coincidental. Dynamic light scattering indicates that free SDS micelles coexist with AM-MAPTAC-10/SDS complexes at this concentration. Thus, the monomeric SDS concentration should match the CMC_p, reasonably approximated to be near 8 mM, and the ionic strength should be at least that large. That, together with the systematic deviations from DLVO behavior at small and large apparent separation distances, lead to the conclusion that the data correspond to a long-range electrosteric force that decays approximately exponentially.

The other prominent feature of the normalized force curves at 2 × CMC is the reappearance of an adhesion force upon surface separation. On average, the adhesive minimum has a depth of -0.2 ± 0.09 mN/m and occurs at approximately 30 nm apparent separation distance. A rather sudden expansion of the adsorbed layer occurs when the compression is reduced during separation. This occurs just below 10 nm apparent separation distance, as most clearly seen on a semilogarithmic representation (Figure 7b). This feature was not present in the normalized force curve in the absence of SDS, but it has been reported for precoated AM-MAPTAC-10 layers on mica subsequently exposed to SDS.[35] A plausible explanation is that SDS is

(35) Kjellin, M.; Claesson, P. M.; Audebert, R. *J. Colloid Interface Sci.* **1997**, *190*, 476.

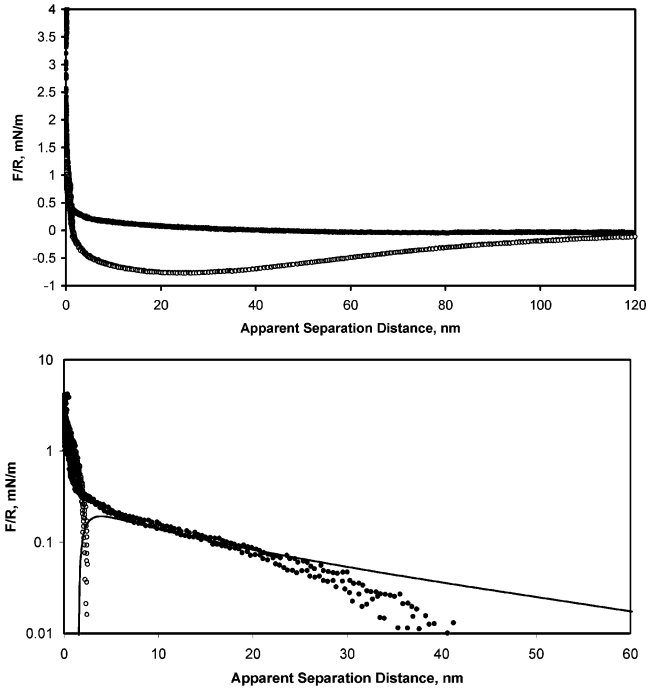

Figure 8. Linear (a) and semilogarithmic (b) plots of the interaction force normalized by radius as a function of apparent surface separation of glass spheres across aqueous 50 ppm AM-MAPTAC-10 solutions without SDS (0.1 mM NaCl background electrolyte) 4 h after rinsing away the 50 ppm AM-MAPTAC-10/2 × CMC SDS solution originally present. Filled and open circles represent the force profiles obtained upon approach and separation, respectively. In the semilogarithmic plot (b) the inward curve is shown together with a fit to DLVO theory with constant surface charge boundary condition (solid line). The following parameters were used in the fitting: apparent surface potential $\Psi_0 = 33$ mV; Debye length $\kappa^{-1} = 30$ nm; Hamaker constant $A = 1 \times 10^{-20}$ J. Data collected at 22 °C. The original layer equilibrated for more than 24 h before rinsing.

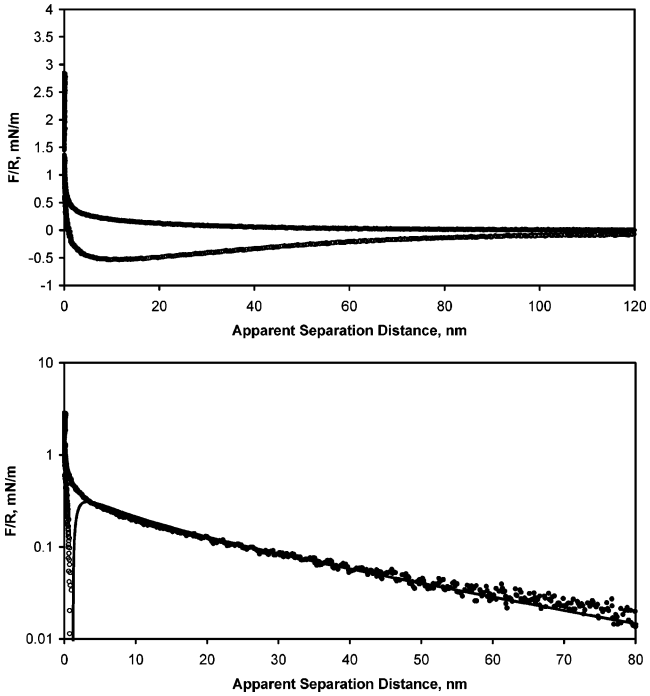

Figure 9. Linear (a) and semilogarithmic (b) plots of the interaction force normalized by radius as a function of apparent surface separation of glass spheres across aqueous 50 ppm AM-MAPTAC-10 solutions without SDS (0.1 mM NaCl background electrolyte). Measured at 22 °C after 48 h of rinsing the same layer as in Figure 8.

removed during compression and then readsorbs into the layer once the compressional pressure has been sufficiently reduced.

That the long-range force measured at 2 × CMC is not a double-layer repulsion is supported by force measurements performed shortly after washing those adsorbed layers with SDS-free solution. Figure 8 shows normalized forces measured in 50 ppm AM-MAPTAC-10/0.1 mM NaCl solution without SDS approximately 4 h after washing SDS from the system. The departure from electrostatic double-layer force (calculated for the expected 0.1 mM ionic strength) is evident at long range. Thus, the force must be of electrosteric nature at all apparent separation distances plotted. Taken together, Figures 7 and 8 indicate that at 2 × CMC the adsorbed layers are highly extended. The high extension of the layers together with the low total surface excess concentration measured by optical reflectometry create favorable conditions for bridging attraction and produce the observed adhesion. As will be noted below, the data measured after 4 h of washing do not represent the final state of the adsorbed layer. It is notable that the adhesion was strongest in the case of 4 h washed layers that had not yet relaxed to their final state. The adhesive minimum was -0.75 ± 0.05 mN/m during this transient state of SDS removal from a mixed layer.

After 48 h of washing the layers in 50 ppm AM-MAPTAC-10/0.1 mM NaCl solution, the adsorbed layers returned to a conformation that is similar to that originally adopted when they first adsorbed to the bare surfaces from 50 ppm AM-MAPTAC-10/0.1 mM NaCl solution. Normalized forces for the exhaustively washed layers, plotted in Figure 9, resembled the original forces that were plotted in Figure 3. The long-range force is consistent with double-layer repulsion between spherical surfaces (with 37 mV apparent surface potential) and the expected ionic strength of 0.1 mM. Deviations from the DLVO behavior appeared at just under 10 nm apparent separation distance.

The adhesive well for the washed layer (-0.5 ± 0.05 mN/m) was similar to that of the original adsorbed layer. The qualitative shape of the force curve measured on separation also returned to its original form. The layer expansion step that appeared in the force curve measured upon separation in the 2 × CMC system disappeared after washing. The similarity in adsorbed amount and in surface forces for the original and the washed layers suggests that the layers return to their original conformation after experiencing a series of dramatic changes in composition and structure.

Interpreting the Effect of SDS Concentration on Adhesion and Layer Structure. Adhesion was only observed in the absence of SDS and in the presence of excess SDS (2 × CMC). The optical reflectometry data indicated a low adsorbed amount under those conditions. No adhesion was observed when the bulk solution contained either 0.1 × CMC or 0.5 × CMC SDS, where the adsorbed amounts were large. It is particularly interesting that the adhesion disappeared under 0.1 × CMC conditions, where the solution was thermodynamically driven to phase separate but where repulsive interaggregate forces rendered the solution a colloidally stable suspension of SDS/AM-MAPTAC-10 aggregates. Consistent with this colloidal stability, the forces between adsorbed layers were repulsive at all separation distances.

In the absence of SDS, double-layer forces operated at apparent separation distances larger than approximately

20 nm and bridging adhesion occurred when the surfaces were separated. Furthermore, the adsorbed amount was small. These results indicate that the adsorbed layers are thin and leave a significant fraction of the total glass surface area accessible to bridging chains.

Adhesion also occurred in the 2 × CMC system. The adsorbed amount in that system was also small. In contrast to the SDS-free system, the long-range force was inconsistent with the electrostatic double-layer repulsion, indicative of long-range electrosteric forces. The small adsorbed amount and large layer extension suggest that the layer consists of highly stretched, yet widely spaced, SDS/AM-MAPTAC-10 complexes. The stretching and spacing result from repulsions among the excess of negative charge on the SDS-saturated polyelectrolyte chain. When two such surfaces come into contact, the complexes anchored on opposite surfaces interdigitate and bridge the gap. One may speculate that the qualitatively different form of the adhesion force curve at 2 × CMC reflects the redistribution of SDS in the mixed adsorbed layer as the gap increases. For AM-MAPTAC-10 to bridge the gap, some SDS must be stripped off the polyelectrolyte in order for it to adsorb electrostatically to the negatively charged glass surface.

Reversibility of Coadsorption. Although AM-MAPTAC-10 adsorbs effectively irreversibly on silica or glass in the absence of SDS and the structure of the layer is affected by how the layer build-up occurs (stepwise increase in polyelectrolyte concentration or direct adsorption from a more concentrated polyelectrolyte solution), adsorbed layers that form in SDS mixtures with AM-MAPTAC-10 respond reversibly to changes in the SDS concentration. When these behaviors are observed, it is suggested that the reversible behavior in the presence of surfactants can be attributed to the solubilization of polymer train segments by bound surfactants.[11−13] Train solubilization decreases the net activation barrier against polymer desorption and mobilizes the adsorbed polymers.

This behavior should be compared to that observed for other type I systems where the surfactant and polymer associate in solution and the surface is selective for the polymer. Braem and co-workers examined a system of SDS with nonionic poly(ethylene oxide)-*b*-(propylene oxide)-*b*-(ethylene oxide) triblock copolymers (PEO−PPO−PEO) and silica surfaces.[4,11] The SDS/PEO−PPO−PEO/silica system behaved similarly to the current system: polymer adsorbed irreversibly in the absence of surfactant, but mixed layers responded reversibly to changes in surfactant concentration. In contrast, Berglund and co-workers found strongly path-dependent coadsorption in mixtures of SDS with cellulosic polymers on silica surfaces.[13] With both PEO−PPO−PEO and cellulosic polymers, weaker nonelectrostatic interactions dominate both the adsorption to silica and the binding to SDS. Yet, why does the SDS/PEO−PPO−PEO/silica system resemble the SDS/AM-MAPTAC-10/silica system in its reversible response to SDS concentration changes while the SDS/cellulosic/silica systems do not?

Three types of interactions need to be considered: the surfactant−surface repulsion, surfactant−polymer attraction, and polymer−surface attraction. In each surfactant/polymer/surface system considered, the electrostatic repulsion between SDS and silica is similar. SDS has a very high affinity for PEO−PPO−PEO, as evident in its low critical CAC. The CAC values for SDS binding to PEO−PPO−PEO[4] and to hydroxypropyl cellulose (HPC)[12] are 0.03 × CMC and 0.2 × CMC, respectively. On the basis of CAC measurements, SDS has a lower binding affinity for HPC than for PEO−PPO−PEO. The electrostatic binding of SDS to AM-MAPTAC-10 is also strong, and the CAC is estimated to be 0.01 × CMC.[16] The difference in coadsorption reversibility between these systems must lie in the ability of electrostatic repulsions originating from the negatively charged silica surface to strip SDS off of the adsorbing polymer in the immediate vicinity of the solid surface. With the very high binding affinity of SDS for PEO−PPO−PEO and for AM-MAPTAC-10, these electrostatic repulsions do not completely strip SDS from PEO−PPO−PEO or AM-MAPTAC-10 segments. Thus, segments that would otherwise become trains are solubilized by bound SDS to become loop or tail segments. By shifting the balance of segments residing in trains vs loops or tails in favor of loops and tails, the overall activation barrier against polymer desorption or rearrangement is decreased.

Given the relatively lower binding affinity of SDS for HPC, the surfactant is more easily stripped from the cellulosic backbone, allowing a greater fraction of segments to remain bound as trains. The mobilization is less effective due to electrostatic stripping of surfactant away from the silica surface. Berglund and co-workers considered both HPC and hydrophobically modified hydroxyethylcellulose (hmHEC). The latter showed strongly hysteretic adsorption, although the CAC was very low. At first glance, this would appear to contradict the trend. The CAC for SDS with hmHEC is only 0.005 × CMC, indicating a very high binding affinity. Nevertheless, this high affinity is due to the presence of a small number of hexadecyl hydrophobes substituted along the polymer backbone. The backbone, most of which is unsubstituted, is itself surface active on silica. Thus, the SDS is still easily stripped off of the cellulosic backbone and the polymer backbone still adsorbs too tenaciously to allow the adsorbed layer to respond to changes in SDS concentration.

The inability of surfactant to solubilize polymer train segments also leads to strongly path-dependent coadsorption in a type IV system where surfactant and polymer do not bind in solution and the surface is nonselective. An example is the CTAB/polylysine/silica system. Without any polymer−surfactant binding, there is no polymer mobilization and the activation barrier against polymer desorption remains effectively insurmountable. Such layers do not respond reversibly to changes in surfactant concentration.

Conclusions

In the absence of SDS, AM-MAPTAC-10 forms relatively thin layers on silica (glass) that leave the surface accessible to bridging chains from opposing surfaces. The long-range force between surfaces with adsorbed AM-MAPTAC-10 is dominated by electrostatic double-layer repulsion at apparent separation distances greater than approximately 10−20 nm.

Complexation of AM-MAPTAC-10 with SDS at concentrations below the CMC produces thick layers containing large amounts of adsorbed material. Electrosteric forces dominate at apparent separation distances as large as 40−80 nm. Enhanced adsorption occurs at 0.1 × CMC, where large SDS/AM-MAPTAC-10 aggregates form in a thermodynamically unstable but colloidally stable suspension. Enhanced adsorption also occurs at 0.5 × CMC, where the solution contains thermodynamically stable complexes of surfactant with a single polyelectrolyte chain. The large surface coverage prevents adhesion between opposing surfaces under these conditions. The absence of adhesion between surfaces coated with SDS/AM-MAPTAC-10 aggregates at 0.1 × CMC is consistent with

the existence of colloidal forces that prevent the large aggregates in solution from coalescing into macroscopically separated liquid phases.

Adsorption decreases considerably at 2 × CMC, yet SDS-saturated complexes form highly extended layers stabilized by electrostatic repulsions among bound SDS. The areal density of adsorbed complexes is evidently quite low, and bridging between opposing surfaces again produces adhesion.

Optical reflectometry and surface force measurements indicate that mixed adsorbed layers of SDS and AM-MAPTAC-10 on silica respond reversibly to changes in the concentration of SDS in the bulk AM-MAPTAC-10/SDS solution, although AM-MAPTAC-10 adsorption is effectively irreversible in the absence of SDS. This lack of coadsorption hysteresis is probably attributable to the high binding affinity of SDS for AM-MAPTAC-10. Strongly bound SDS solubilizes and mobilizes polyelectrolyte segments that would otherwise be bound to the surface as trains.

Acknowledgment is made to the donors of the Petroleum Research Fund, administered by the American Chemical Society, for partial support of this research. This material is also based in part on work supported by the National Science Foundation under Grant INT-0217721.

LA035752W